PLOS | CURRENTS OUTBREAKS

Phylodynamic Analysis of Ebola Virus in the 2014 Sierra Leone Epidemic

October 24, 2014 · *Research Article*

Citation

Volz E, Pond S. Phylodynamic Analysis of Ebola Virus in the 2014 Sierra Leone Epidemic. PLOS Currents Outbreaks. 2014 Oct 24 . Edition 1. doi: 10.1371/currents.outbreaks.6f7025f1271821d4c815385b08f5f80e.

Tweet

Authors

Erik Volz

Department of Infectious Disease Epidemiology, Imperial College London, London, United Kingdom.

Sergei Pond

Medicine, University of California San Diego, San Diego, CA, USA.

Abstract

Background: The Ebola virus (EBOV) epidemic in Western Africa is the largest in recorded history and control efforts have so far failed to stem the rapid growth in the number of infections. Mathematical models serve a key role in estimating epidemic growth rates and the reproduction number (R0) from surveillance data and, recently, molecular sequence data. Phylodynamic analysis of existing EBOV time-stamped sequence data may provide independent estimates of the unobserved number of infections, reveal recent epidemiological history, and provide insight into selective pressures acting upon viral genes.

Methods: We fit a series mathematical models of infectious disease dynamics to phylogenies estimated from 78 whole EBOV genomes collected from distinct patients in May and June of 2014 in Sierra Leone, and perform evolutionary analysis on these genomes combined with closely related EBOV genomes from previous outbreaks. Two analyses are conducted with values of the latent period that have been used in recent modelling efforts. We also examined the EBOV sequences for evidence of possible episodic adaptive molecular evolution during the 2014 outbreak.

Results: We find evidence for adaptive evolution affecting L and GP protein coding regions of the EBOV genome, which is unlikely to bias molecular clock and phylodynamic analyses. We estimate R0=2.40 (95% HPD:1.54-3.87) if the mean latent period is 5.3 days, and R0=3.81, (95% HPD:2.47-6.3) if the mean latent period is 12.7 days. The estimated coefficient of variation (CV) of the number of transmissions per infected host is very high, and a large proportion of infections yield no transmissions.

Conclusions: Estimates of R0 are sensitive to the unknown latent infectious period which can not be reliably estimated from genetic data alone. EBOV phylogenies show significant evidence for superspreading and extreme variance in the number of transmissions per infected individual during the early epidemic in Sierra Leone.

Funding Statement

EMV and SLKP are supported by NIH Models of Infectious Disease Agent Study (MIDAS) grant U01GM110749. Computational work was supported by the UCSD Center for AIDS Research (BIT Core, P30

AI036214). EMV was partly supported by the UK Medical Research Council (MRC) and the UK Department for International Development (DFID) under the MRC/DFID Concordat agreement. The funders had no role in study design, data collection and analysis, decision to publish, or preparation of the manuscript.

Introduction

The 2014 Ebola virus in Western Africa is the largest Ebola epidemic in history and the number of infections continues to grow exponentially. The unprecedented rate of growth has negatively impacted the quality of epidemiological surveillance and has made it difficult to map and characterize the spread of the epidemic [13] . As local health and surveillance systems are overwhelmed, an unknown proportion of cases are unreported, are not isolated, and do not receive adequate treatment. Predictive modelling and evaluation of intervention efforts is also hampered by the rapid rate of increase and imperfect case reporting.

In the absence of complete surveillance data and contact tracing, mathematical models[20] have provided valuable insights into the rate of epidemic growth and the reproduction number (R_0). The reproduction number is a useful parameter for characterizing the difficulty of eradication. Early analyses based on case reporting by the World Health Organization (WHO) indicated thatR_0 differed substantially between countries[19,17] . In some instances, estimates of R_0 based on different models are not in agreement, implying that they are sensitive to the assumptions of the mathematical framework used, and the exact data sets used for parameter estimation. Althaus[19] estimated $R_0 = 2.53$ (2.41-2.67) for Sierra Leone based on WHO case reports through late August 2014, whereas Fisman et al. [17] estimated $R_0 = 8.3$ for Sierra Leone using a similar data set. More recently, Towers et al.[18] estimated $R_0 = 1.2$ (1.0,1.5) for Sierra Leone using a longer timeseries of case reports and a model with time-dependent reproduction numbers. And, the WHO Ebola Response Team[1] presents an estimate of $R_0 = 2.02$ (1.789-2.26) for Sierra Leone, which additionally makes use of new information about the incubation period and serial interval for the current epidemic. The analysis by Althaus modeled the natural history of infection by including a mean 5.3 day latent period before cases become infectious, whereas the analysis by Fisman et al. used a much longer latent period, but did not explicitly consider the lack of infectiousness during the latent period.

We conduct a phylodynamic[21] analysis of 78 Ebola virus genetic sequences discussed in Gire et al.[16]. These data provide an independent source of information about epidemic growth rates and R_0 and may corroborate previous estimates based on case reporting data. To examine the sensitivity of R_0 estimates to the unknown latent period, we repeat our analysis with two values (5.3 and 12.7 days) which have been estimated from previous Ebola outbreaks.

Recently, Stadler et al.[34] conducted a similar phylodynamic analysis of the same data. We conclude our analysis with a discussion of the primary differences in the analytic approach and findings of these two studies.

An advantage of phylodynamic analysis is that estimates are robust to incomplete sampling of cases, and the proportion of cases which are unreported does not enter directly into our model[24] . Sequence data may also be informative about epidemiological parameters where standard surveillance data are unhelpful. Previous phylodynamic analyses have shown how sequence data can be highly informative about who infected whom[26] and risk factors for transmission[25]. In addition to R_0, we estimate parameters that describe heterogeneity in transmission rates between infected individuals. Fitting these models allows us to characterize superspreading as well as estimate the proportion of cases which do not yield secondary infections.

We also examine the virus genomes for evidence of natural selection, which can potentially bias phylodynamic analyses by violating assumptions of neutral evolution. Because the primary analysis of EBOV isolates [16] found a large number of non-synonymous mutations in whole length genomes, and because strong selective pressures can bias molecular clocks[10,11], and violate the assumptions of the standard coalescent process[9], we performed an exhaustive analysis of all genes in the EBOV genome for evidence of episodic diversifying natural selection using sensitive codon-substitution evolutionary models.

Methods

Data. We conduct a secondary analysis of EBOV phylogenies presented by Gire et al.[16] Samples were collected for whole-genome deep sequencing from 78 patients between 25 May and 20 June in Sierra Leone. In situations where multiple samples were available for a single patient, only the first sample was used in the phylogenetic analysis. Dates of common ancestry for all pairs of samples were estimated with using Bayesian relaxed clock methods [28] . Further details of the sequencing protocol and models used for phylogenetic analysis can be found in Gire et al. [16] This procedure yields a sample from the posterior distribution of dated phylogenies, from which we sampled 1,000 trees to make computation tractable.

For molecular selection analyses, we augmented the 2014 outbreak sequences with 17-37 (depending on the gene) additional isolates from previous EBOV outbreaks (1976-2007), which were also included in the original Bayesian relaxed clock analysis [16].

Cumulative numbers of cases reported by WHO were acquired from https://github.com/cmrivers/ebola on September 13, 2014.

Models. The starting point for the analysis is the SEIR model, which has previously been applied to EBOV outbreaks [29,30]and has recently been applied to the 2014 epidemic [19] .

The parameter β will be the transmission rate per infectious individual, γ_E will be the rate that infected progress from the latent period to the infectious period, and $\gamma_I$will be the rate that infectious cases are removed due to death and burial or by effective isolation and treatment. The ordinary differential equations for the deterministic SEIR model are:

$$\frac{\mathrm{d}}{\mathrm{d}t}E = \beta IS\,/\,N - \gamma_E$$
$$\frac{\mathrm{d}}{\mathrm{d}t}I = \gamma_E E - \gamma_I I$$

Fig. 1: SEIR equations.

These equations describe the dynamics of the number E exposed non-infectious individuals and the number of infectious individuals I. We make the approximation that the majority of the population is in the susceptible category ($S/N \approx 1$) for this and subsequent models, such that an equation for the dynamics of S is not needed.

In order to estimate heterogeneity in transmission rates, we extend the SEIR model to include two infectious categories, I_l and I_h. When the latent period ends, a case progresses to the category I_h with probability p and category I_l with probability $1-p$. According to this model, transmissions only occur from the category I_h. By changing the parameter p, the variance in transmissions per infectious case can be made arbitrarily large. The deterministic equations are:

$$
\begin{aligned}
\frac{\mathrm{d}}{\mathrm{d}t}E &= \beta I_h S/N - \gamma_E E \\
\frac{\mathrm{d}}{\mathrm{d}t}I_l &= (1-p)\gamma_E E - \gamma_I I_l \\
\frac{\mathrm{d}}{\mathrm{d}t}I_h &= p\gamma_E E - \gamma_I I_h
\end{aligned}
$$

Fig. 2: ODE SEIIR equations.

We will refer to this as the ODE SEIIR model.

A stochastic version of the SEIIR model was also fitted in order to account for any bias due to noisy dynamics during the early exponential growth phase of the epidemic. The equations for this model are given by the following stochastic differential equations:

$$\begin{aligned}
\frac{\mathrm{d}}{\mathrm{d}t}E &= \beta I_h S/N - \gamma_E E + \frac{\mathrm{d}W_1}{\mathrm{d}t}\sqrt{\gamma_E E} + \frac{\mathrm{d}W_2}{\mathrm{d}t}\sqrt{\beta I_h S/N} \\
\frac{\mathrm{d}}{\mathrm{d}t}I_l &= (1-p)\gamma_E E - \gamma_I I_l + (1-p)\frac{\mathrm{d}W_1}{\mathrm{d}t}\sqrt{\gamma_E E} + (1-p)\frac{\mathrm{d}W_3}{\mathrm{d}t}\sqrt{\gamma_I I} \\
\frac{\mathrm{d}}{\mathrm{d}t}I_h &= p\gamma_E E - \gamma_I I_h + p\frac{\mathrm{d}W_1}{\mathrm{d}t}\sqrt{\gamma_E E} + p\frac{\mathrm{d}W_3}{\mathrm{d}t}\sqrt{\gamma_I I}
\end{aligned}$$

Fig. 3: SDE SEIIR equations.

where $W_i(t)$ are independent Wiener (standard Brownian motion) processes, and $I = I_h + I_l$. This system accounts for noise in incidence and deaths, but does not account for noise in the composition of I into the I_l and I_h categories because of the difficulty of fitting such a system to data. Note that the stochastic terms in the equations for I_l and I_h are the same and multiplied by $1-p$ and p respectively. We will refer to this model as the SDE SEIIR model. The euler method with a time step of one day was used to simulate trajectories from the SDEs.

Statistical analysis. The epidemiological models were fitted to EBOV phylogenies using the rcolgem package in R[22,23], which computes the likelihood of epidemiological parameters given a phylogeny. When fitting the ODE and SDE SEIIR models, likelihoods were calculated for each phylogeny with the boundary condition that each sample is a superspreader with probability p, which is estimated. Models were fitted using a Bayesian Markov chain within Metropolis (MCWM) algorithm[15] , which integrates over the distribution of phylogenies previously estimated in Gire et al.[16] . This algorithm was implemented by customizing the *mcmc* package in R. At each step k of the MCWM algorithm, the likelihood of the set of trees $\{\mathcal{G}_i\}_{i=1}^{n}$ given a solution $\mathcal{M}_k$ of the epidemiological model is approximated by $\widehat{\mathcal{L}}_k = \frac{1}{n}\sum_{i=1}^{n} P(\mathcal{G}_i|\mathcal{M}_k)$ The n genealogies used in the approximation are drawn uniformly at random from the distribution estimated by Gire et al. [16] If fitting a stochastic model, a double-marginalization is required over genealogies and simulations of the stochastic model. Such a Markov chain will sample the posterior distribution regardless of the choice of sample size n, however the value used will influence the efficiency of the algorithm. We chose $n = 4 \times 16 = 64$ for ODE models and $5 \times 64 = 320$ for SDE models to match the architecture of our high performance computing cluster.

In the SEIR model, two parameters were estimated: R_0 and the time t_0 when the epidemic was initiated in Sierra Leone. In the ODE SEIIR and SDE SEIIR model, the parameter p was also estimated, which controls the proportion of cases in I_h. A diffuse lognormal prior (mean 3.2, standard deviation 2.5) was used for R_0, a uniform(0,1) prior was used for p, and a normal prior for t_0 with mean April 23, and standard deviation of 6 days (based on the results by Althaus[19]).

We compared models using the approximate AICM method[32]. AICM is a summary statistic for the goodness of model fit for Bayesian analyses, and is analogous to the Akaike information criterion (AIC[8]) used for model selection in the maximum likelihood framework. AICM was calculated using Tracer1.6[14] . At least two MCWM chains were sampled for each model and combined with 20% of samples removed for burn-in and effective sample sizes were computed to confirm adequate sample size.

The reproduction number was calculated using $R_0 = \beta / \gamma_I$ for the SEIR model and $R_0 = p\beta / \gamma_I$ for the SEIIR models. The coefficient of variation (CV) was computed under the assumption that if an individual is infectious, the number of transmissions has a geometric distribution with parameter $\gamma_I / (\gamma_I + \beta)$. For a geometric distribution under the SEIR model, CV=$\sqrt{(R_0+1)/R_0}$. According to the SEIIR model, an individual is infectious with probability p, which yields CV =$\sqrt{(R_0(2/p-1)+1)/R_0}$.

Selection analyses. We extracted sequences spanning the complete lengths of the seven annotated genes of EBOV[16] and fitted several evolutionary models to multiple sequence alignments (MSAs) using fixed maximum clade credibility (MCC) trees computed from previous BEAST runs. MSAs were easily obtained because of the lack of indel variation in EBOV. We used sensitive methods for detecting episodic diversifying selection at the level of individual sites (mixed effects model of evolution[5]), individual branches (branch-site random effects likelihood, BSREL[6]), and a modification of the BSREL to test for gene-wide selection operating on the (monophyletic) clade of 2014 EBOV sequences. Let ω denote the ratio of non-synonymous to synonymous substitution rates. Briefly, whereas the original BSREL method describes the evolutionary process by fitting a model with a mixture of three separate ω values for each tree branch, we partitioned the tree into the foreground (the 2014 Western Africa EBOV clade) and background (all other branches) segments, and fitted two 3-bin ω distributions jointly to all the branches in each partition. A likelihood ratio test of the unconstrained model versus the null model where all $\omega \leq 1$ (i.e. negative selection or neutral evolution) was used to establish significance for evidence of diversifying positive selection affecting a proportion of sites along a proportion of 2014 EBOV lineages. All analyses have been implemented and run using HyPhy v2.12 [7].

Results

Table 1 shows parameter estimates based on four epidemiological models. Estimates of R_0 based on the simple SEIR model are similar to those based on the ODE SEIIR model (posterior median $R_0 = 2.14, 2.10$ respectively), however the SEIR model does not provide an estimate of heterogeneity in transmission rates. The stochastic SEIIR model gives similar estimates to the deterministic SEIIR model, but wider credible intervals, and a slightly larger R_0 of 2.40 (95% HPD:1.54-3.87). These estimates are broadly consistent with the previously published estimates in Althaus [19] and by the WHO Response Team [1] which were based on WHO case reporting in Sierra Leone.

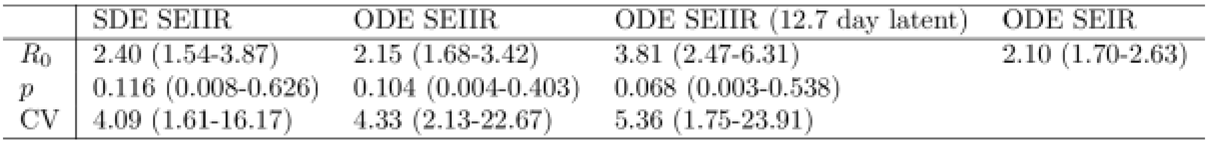

	SDE SEIIR	ODE SEIIR	ODE SEIIR (12.7 day latent)	ODE SEIR
R_0	2.40 (1.54-3.87)	2.15 (1.68-3.42)	3.81 (2.47-6.31)	2.10 (1.70-2.63)
p	0.116 (0.008-0.626)	0.104 (0.004-0.403)	0.068 (0.003-0.538)	
CV	4.09 (1.61-16.17)	4.33 (2.13-22.67)	5.36 (1.75-23.91)	

Table 1. Posterior median and 95% credible intervals based on four epidemiological models.

Unless stated otherwise, each model assumed a mean 5.3 day latent period.

Estimates of R_0 are sensitive to the latent period which could not be estimated from the genetic data alone. Published estimates of the duration of the latent period based on earlier Ebola outbreaks are highly variable [31] , but we present results based on two values that have been used in recent modelling studies of the current epidemic in Western Africa. If the latent period is a mean of 12.7 days, the fitted ODE SEIIR model provides an estimate of $R_0 = 3.8$(95% HPD:2.47-6.31).

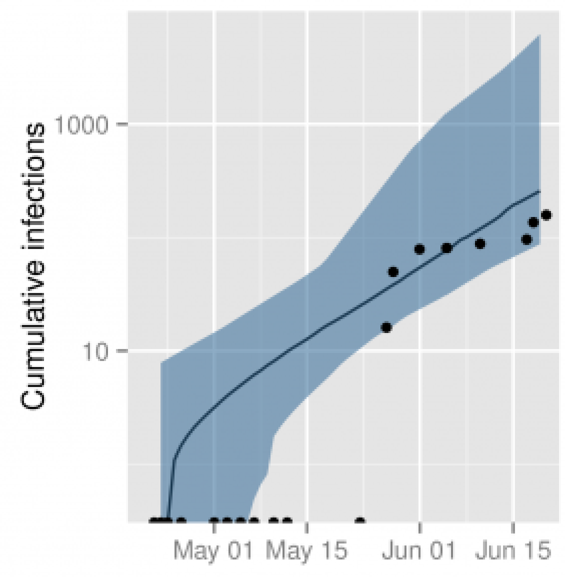

Fig. 4: Cumulative number of symptomatic infections through time.

The estimated cumulative infections through time using the ODE SEIIR model. The shaded region represents the 95% HPD region and the line is the median. The points represent the cumulative number of infections (confirmed and probable) reported by WHO.

Figure 4 shows the estimated cumulative number of infections through time as predicted by the ODE SEIIR model with $1/\gamma_E = 5.3$ days. These estimates, while imprecise, are consistent with reported cases by WHO which were not used for model fitting. The slightly larger number of cases predicted by the model may in part reflect under-reporting of cases in the WHO data.

We find strong evidence for superspreading. The fitted SEIIR models which account for supsperspreading have higher median posterior log likelihoods of -346.9 versus -380.1 for the SEIR model. The ODE SEIIR model is also superior to the SEIR model by the AICM criterion. For two distinct Markov chain samples, we find ΔAICM=-38.7 and -25.6 in favor of the ODE SEIIR model.

In all fits of the SEIIR model, the estimated proportion of cases in the high transmission rate category is less than 63% and posterior median estimates are approximately 10%. Figure 5 shows the EBOV phylogeny with maximum posterior probability. Branches are colored with the probability that the virus lineage inhabits a superspreading host. The superspreader lineage probabilities are based on the median posterior parameter estimates with the ODE SEIIR model. When a lineage occupies a superspreading host (shaded red), it is much more likely to undergo a coalescent event, that is, to have common ancestry with other sampled lineages. This process yields phylogenies with very imbalanced topologies. It also introduces correlation between the lengths of neighboring ancestral and daughter branches, as a lineage in a superspreading host is likely to undergo several coalescent events in short succession.

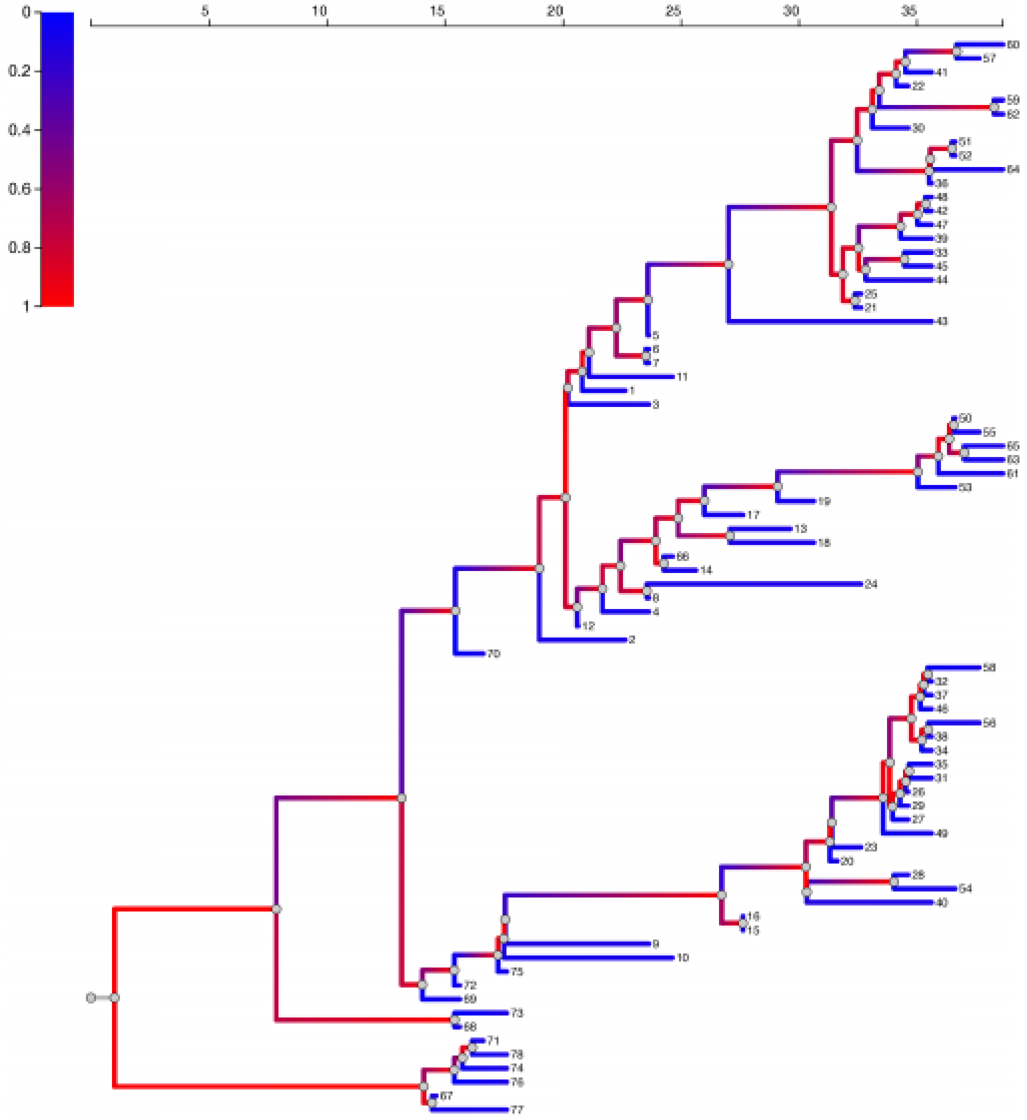

Fig. 5: EBOV phylogeny.

Ebola virus phylogeny based on samples from 78 patients in Sierra Leone showing superspreading. The color of branches represents the estimated probability that the virus lineage inhabits a superspreading host. This phylogeny had the maximum sampled posterior probability in the phylogenetic analysis in Gire et al.[16] Estimates are based on the median posterior parameter estimates with the ODE SEIIR model.

Selection analyses. Table S1 provides an overview of codon-based selection analyses of the seven EBOV protein coding regions. There is a notable variation in nucleotide level diversity across genes (total tree length), with the glycoprotein (GP) showing the highest diversity. About 0.5% of branch-site combinations in the long RNA polymerase (L) gene appear to be under strong diversifying selection ($\omega > 100$) in the 2014 clade, whereas the entirety of sequence evolution in the GP gene is comprised of non-synonymous changes ($\omega > 1$at 100% of branch-site combinations). The remaining genes do not contain significant positive selection signal.

When we asked which individual sites showed evidence of episodic diversification (using the MEME[5] method with p-value < 0.95), sites 388 and 389 in the heavily glycosylated mucin-like domain of GP, and sites 1396, 1492, 1722 in L were identified.

Discussion

Phylodynamic analysis of EBOV sequences provides a new perspective on R_0 and epidemic growth rates that is independent of previous analyses based on WHO case reports. Previous analyses have reached divergent conclusions about R_0 in Sierra Leone, and our estimates are consistent with previous analyses in Althaus[19] and by the WHO Ebola Response Team[1] if assuming a short latent infection period, but slightly larger if assuming a longer latent infection period. Our results are sensitive to the early evolutionary history of the Sierra Leone EBOV, much of which occurred before the first WHO case reports. Thus, the discrepancy of our results with the studies by Towers et al.[18], who reported smaller values of R_0, may be due the decrease in epidemic growth rates observed in July and August. Estimates of R_0 are very sensitive to the unknown duration of the latent period which can not be estimated from genetic data alone. Recently, the WHO Ebola Response Team published its first estimates of the incubation period and serial intervals for the 2014 epidemic[1], and found a mean incubation period of 11.4 days. This suggests that R_0 is closer to the upper bound of our range of estimates (2.10-3.85). Stadler et al.[34] recently estimated R_0=2.18 (95% HPD 1.24-3.55) using the same genetic data used in our analysis. These results are close to our findings if comparing similar models (SEIR and BDEI) and similar incubation periods. The credible intervals in the analysis by Stadler et al.[34] are much wider because a diffuse prior was used for the latent period, whereas we tested the sensitivity to this parameter by repeating the analysis with the latent period fixed at different values.

While we find that it is not possible to estimate the latent period from genetic data alone, Stadler et al.[34] have conducted a phylodynamic analysis of the same EBOV data and estimated a mean incubation period (assumed equivalent to the latent period) of 4.92 days (95% HPD 2.11-23.20). Stadler et al.'s inference of incubation periods was made possible by using additional information, namely the times of genetic sequence sample collection, which were assumed to be collected at a constant per-capita rate. By calibrating the exponential growth rates of the epidemic to match the rate of sample collection, other parameters are rendered identifiable. Incorporating a model of the sampling process into phylodynamic inference can greatly increase statistical power[24], however it can also bias estimates if the sampling process is misspecified. We do not find evidence that the sampling rate was constant as required by the analysis in Stadler at al.[34], but rather that it increased steadily over the sample collection period. By comparing the cumulative number of infections reported by WHO to the cumulative number of samples collected, we find that the sampling rate varied from 20% early in the epidemic to 70% near the end of the sample collection period. An alternative to using times of sample collection to calibrate growth rates would be to use the WHO case reports. Unfortunately, there is very little overlap between the time-stamped EBOV phylogenies and WHO case reports because all samples were collected during the early portion of the epidemic.

In contrast to the analysis by Stadler et al.[34] , we find statistically significant support for a model which features superpreading (heterogeneous transmission rates). These divergent findings may be due to differences in the population genetic models used (coalescent and birth-death-sampling). The discrepancy may also be due to a different parameterisation of superspreading. The analysis by Stadler et al. required two additional parameters to describe superspreading. We chose a model of superspreading which required only one additional parameter, thereby increasing discriminatory power at the expense of some realism. The quantitative estimates of the CV of the reproduction number may be biased upwards by unrealistic distributional assumptions in our model. It is unlikely that transmission heterogeneity is well described by a mixture of only two transmission rates.

It is possible to characterize superspreading patterns from virus phylogenies because the variance in transmissions per case alters the genetic relatedness of a random sample of EBOV sequences[27]. The EBOV phylogenies are highly imbalanced, and neighbouring branch lengths are highly correlated. We hypothesize that these features are a consequence of high variance in transmission rates, and we have proposed an epidemiological population genetic model that reproduces these features. Our epidemiological model of superspreading lacks some realism, however our parameterisation of the transmission process allows us to easily estimate variance in transmission rates.

High variance in transmission rates may hamper contact tracing efforts, since a single missed contact may trigger a sizeable outbreak. Epidemics which feature a highly skewed distribution of transmissions per infected individual differ substantially from epidemics where the number of transmissions cluster around R_0 [3,2] . In epidemics with many superspreading events, the probability of epidemic extinction is greater, and the probability that a single introduction into a susceptible population will trigger an epidemic is also lower. But, when outbreaks do occur, they are more explosive and contact tracing may be more difficult. Furthermore, intervention strategies that are targeted towards individuals with higher transmission risk are likely to be more effective in epidemics with superspreading events. We estimate that a small proportion of infected cases are responsible for a majority of transmissions and a large proportion of infections yield no transmissions.

Our molecular selection analyses suggest that episodic diversifying selection may be operating on L and GP genes. When analysing recent viral isolates, much of the selection signal could be driven by overall maladaptive substitutions along terminal branches due to intra-host evolution [4]. When additional isolates become available, some of the techniques for filtering out such substitutions (e.g. analysing only internal branches [4]) may prove fruitful. The functional importance of sites subject to such forces remains to be elucidated.

Many factors contribute to the uncertainty of our findings, including uncertainty in the EBOV phylogenies, dates of common ancestry, and inherent noisiness of the epidemic process during the early period of exponential growth. Our estimates are based on a relatively small sample of EBOV sequences, and much greater precision could be achieved if a larger proportion of cases are sequenced over a longer period of time. Genetic sequence data are only available for the very early portion of the epidemic in Sierra Leone. Estimates may differ in other countries and settings, as well as through time as intervention efforts are scaled up and the population adapts to the growing epidemic. Phylodynamic methods are robust to variable and incomplete sampling of cases, so that virus sequences may be a useful supplement to epidemic surveillance if a growing proportion of cases are not reported to health systems.

Competing Interests

The authors have declared that no competing interests exist.

Acknowledgements

The authors thank Andrew Rambaut for furnishing the EBOV phylogenetic tree data, and Samantha Lycett and Christophe Fraser for valuable suggestions.

Appendix 1

Supporting Tables and Figures

Table S1: Selection analysis.

Selection analysis results on EBOV genes; N, number of sequence; L, number of codons; T, total tree length, expected substitutions/nucleotide site. ω^{2014} is the inferred distribution of the ratio of non-synonymous to synonymous substitution rates under the modified branch-site REL model (see text) on the clade comprising 2014 outbreak isolates (weight of each category is indicated in the parentheses); for the two genes with significant p-values, we also indicate approximate 95% confidence intervals (likelihood profile) for the ω categories with estimates over 1 in square brackets; ω^{other} is the corresponding distribution for the remainder of the tree (pre-2014); p is the p-value for the likelihood ratio test for evidence of episodic diversifying selection anywhere in the 2014 clade.

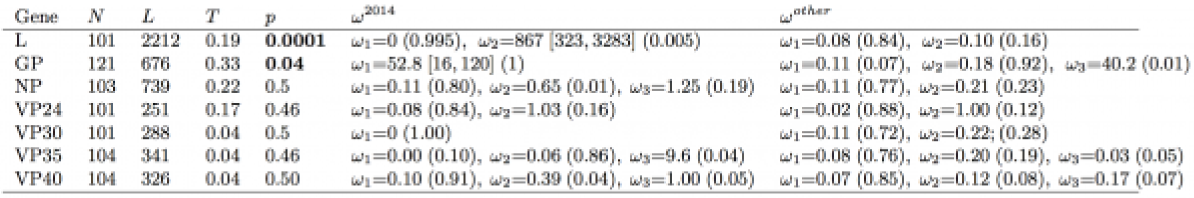

Gene	N	L	T	p	ω^{2014}	ω^{other}
L	101	2212	0.19	**0.0001**	ω_1=0 (0.995), ω_2=867 [323, 3283] (0.005)	ω_1=0.08 (0.84), ω_2=0.10 (0.16)
GP	121	676	0.33	**0.04**	ω_1=52.8 [16, 120] (1)	ω_1=0.11 (0.07), ω_2=0.18 (0.92), ω_3=40.2 (0.01)
NP	103	739	0.22	0.5	ω_1=0.11 (0.80), ω_2=0.65 (0.01), ω_3=1.25 (0.19)	ω_1=0.11 (0.77), ω_2=0.21 (0.23)
VP24	101	251	0.17	0.46	ω_1=0.08 (0.84), ω_2=1.03 (0.16)	ω_1=0.02 (0.88), ω_2=1.00 (0.12)
VP30	101	288	0.04	0.5	ω_1=0 (1.00)	ω_1=0.11 (0.72), ω_2=0.22; (0.28)
VP35	104	341	0.04	0.46	ω_1=0.00 (0.10), ω_2=0.06 (0.86), ω_3=9.6 (0.04)	ω_1=0.08 (0.76), ω_2=0.20 (0.19), ω_3=0.03 (0.05)
VP40	104	326	0.04	0.50	ω_1=0.10 (0.91), ω_2=0.39 (0.04), ω_3=1.00 (0.05)	ω_1=0.07 (0.85), ω_2=0.12 (0.08), ω_3=0.17 (0.07)

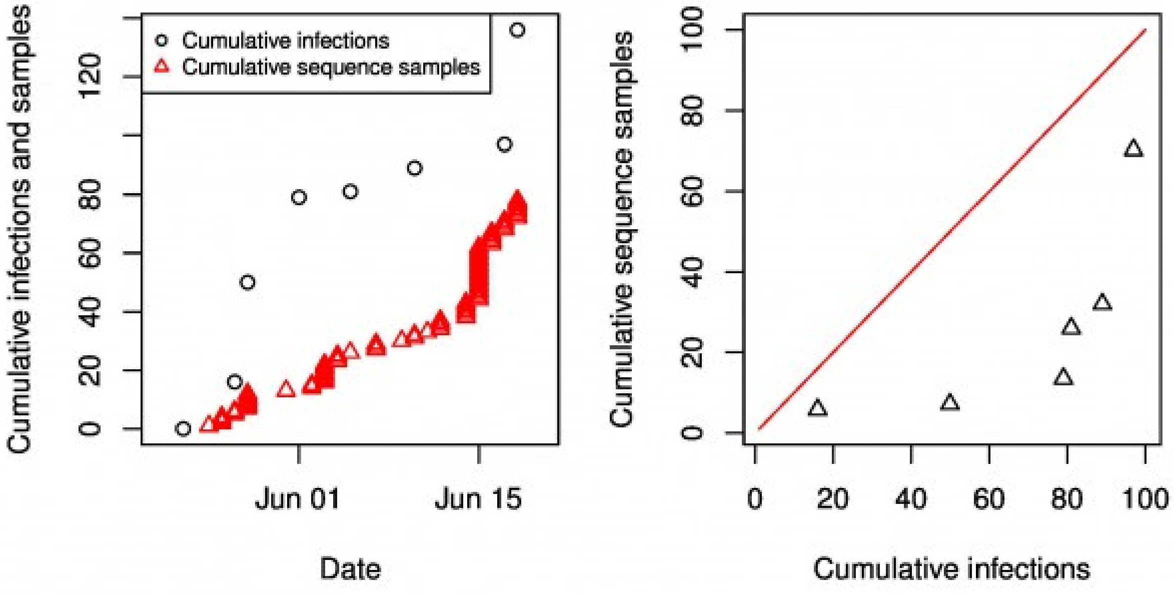

Fig S1: Sampling through time.

Left: The cumulative sequence samples as a function of time are compared to cumulative confirmed and probable cases reported by WHO. Right: The WHO cumulative infections versus the interpolated cumulative number of sequence samples. If the sampling rate was constant, these points would follow a linear trend.

References

1. Ebola Virus Disease in West Africa - The First 9 Months of the Epidemic and Forward Projections. N Engl J Med. 2014 Sep 22. PubMed PMID:25244186.

2. Meyers LA, Pourbohloul B, Newman ME, Skowronski DM, Brunham RC. Network theory and SARS: predicting outbreak diversity. J Theor Biol. 2005 Jan 7;232(1):71-81. PubMed PMID:15498594.

3. Lloyd-Smith JO, Schreiber SJ, Kopp PE, Getz WM. Superspreading and the effect of individual variation on disease emergence. Nature. 2005 Nov 17;438(7066):355-9. PubMed PMID:16292310.

4. Pond SL, Frost SD, Grossman Z, Gravenor MB, Richman DD, Brown AJ. Adaptation to different human populations by HIV-1 revealed by codon-based analyses. PLoS Comput Biol. 2006 Jun 23;2(6):e62. PubMed PMID:16789820.

5. Murrell B, Wertheim JO, Moola S, Weighill T, Scheffler K, et al. (2012) Detecting individual sites subject to episodic diversifying selection. PloS Genet in press.

6. Kosakovsky Pond SL, Murrell B, Fourment M, Frost SD, Delport W, Scheffler K. A random effects branch-site model for detecting episodic diversifying selection. Mol Biol Evol. 2011 Nov;28(11):3033-43. PubMed PMID:21670087.

7. Pond SL, Frost SD, Muse SV. HyPhy: hypothesis testing using phylogenies. Bioinformatics. 2005 Mar 1;21(5):676-9. PubMed PMID:15509596.

8. Akaike H (1974) A new look at the statistical model identification. IEEE Transactions on Automatic Control 19:6: 716–723.

9. O'Fallon BD. A method for accurate inference of population size from serially sampled genealogies distorted by selection. Mol Biol Evol. 2011 Nov;28(11):3171-81. PubMed PMID:21680870.

10. Wertheim JO, Kosakovsky Pond SL. Purifying selection can obscure the ancient age of viral lineages. Mol Biol Evol. 2011 Dec;28(12):3355-65. PubMed PMID:21705379.

11. Wertheim JO, Fourment M, Kosakovsky Pond SL. Inconsistencies in estimating the age of HIV-1 subtypes due to heterotachy. Mol Biol Evol. 2012 Feb;29(2):451-6. PubMed PMID:22045998.

13. Piot P. Ebola's perfect storm. Science. 2014 Sep 12;345(6202):1221. PubMed PMID:25214580.

14. Rambaut A, Suchard M, Xie D, Drummond A (2014). Tracer v1.6. Available from http://beast.bio.ed.ac.uk/Tracer.

15. Andrieu C, Roberts GO (2009) The pseudo-marginal approach for efficient monte carlo computations. The Annals of Statistics : 697–725.

16. Gire SK, Goba A, Andersen KG, Sealfon RS, Park DJ, Kanneh L, Jalloh S, Momoh M, Fullah M, Dudas G, Wohl S, Moses LM, Yozwiak NL, Winnicki S, Matranga CB, Malboeuf CM, Qu J, Gladden AD, Schaffner SF, Yang X, Jiang PP, Nekoui M, Colubri A, Coomber MR, Fonnie M, Moigboi A, Gbakie M, Kamara FK, Tucker V, Konuwa E, Saffa S, Sellu J, Jalloh AA, Kovoma A, Koninga J, Mustapha I, Kargbo K, Foday M, Yillah M, Kanneh F, Robert W, Massally JL, Chapman SB, Bochicchio J, Murphy C, Nusbaum C, Young S, Birren BW, Grant DS, Scheiffelin JS, Lander ES, Happi C, Gevao SM, Gnirke A, Rambaut A, Garry RF, Khan SH, Sabeti PC. Genomic surveillance elucidates Ebola virus origin and transmission during the 2014 outbreak. Science. 2014 Sep 12;345(6202):1369-72. PubMed PMID:25214632.

17. Fisman D, Khoo E, Tuite A. Early Epidemic Dynamics of the West African 2014 Ebola Outbreak: Estimates Derived with a Simple Two-Parameter Model. PLOS Currents Outbreaks. 2014 Sep 8. Edition 1. doi: 10.1371/currents.outbreaks.89c0d3783f36958d96ebbae97348d571.

18. Towers S, Patterson-Lomba O, Castillo-Chavez C. Temporal Variations in the Effective Reproduction Number of the 2014 West Africa Ebola Outbreak. PLOS Currents Outbreaks. 2014 Sep 18. Edition 1. doi: 10.1371/currents.outbreaks.9e4c4294ec8ce1adad283172b16bc908.

19. Althaus CL. Estimating the Reproduction Number of Ebola Virus (EBOV) During the 2014 Outbreak in West Africa. PLOS Currents Outbreaks. 2014 Sep 2. Edition 1. doi: 10.1371/currents.outbreaks.91afb5e0f279e7f29e7056095255b288.

20. Gomes MFC, Pastore y Piontti A, Rossi L, Chao D, Longini I, Halloran ME, Vespignani A. Assessing the International Spreading Risk Associated with the 2014 West African Ebola Outbreak. PLOS Currents Outbreaks. 2014 Sep 2. Edition 1. doi: 10.1371/currents.outbreaks.cd818f63d40e24aef769dda7df9e0da5.

21. Volz EM, Koelle K, Bedford T. Viral phylodynamics. PLoS Comput Biol. 2013;9(3):e1002947. PubMed PMID:23555203.

22. Volz EM. Complex population dynamics and the coalescent under neutrality. Genetics. 2012 Jan;190(1):187-201. PubMed PMID:22042576.

23. Rasmussen DA, Volz EM, Koelle K. Phylodynamic inference for structured epidemiological models. PLoS Comput Biol. 2014 Apr;10(4):e1003570. PubMed PMID:24743590.

24. Volz EM, Frost SD (2014) Sampling through time and phylodynamic inference with coalescent and birth-death models. Journal of the Royal Society Interface. In press.

25. Volz EM, Ionides E, Romero-Severson EO, Brandt MG, Mokotoff E, Koopman JS. HIV-1 transmission during early infection in men who have sex with men: a phylodynamic analysis. PLoS Med. 2013 Dec;10(12):e1001568; discussion e1001568. PubMed PMID:24339751.

26. Didelot X, Gardy J, Colijn C. Bayesian inference of infectious disease transmission from whole-genome sequence data. Mol Biol Evol. 2014 Jul;31(7):1869-79. PubMed PMID:24714079.

27. Donnelly P, Tavaré S. Coalescents and genealogical structure under neutrality. Annu Rev Genet. 1995;29:401-21. PubMed PMID:8825481.

28. Drummond AJ, Suchard MA, Xie D, Rambaut A. Bayesian phylogenetics with BEAUti and the BEAST 1.7. Mol Biol Evol. 2012 Aug;29(8):1969-73. PubMed PMID:22367748.

29. Chowell G, Hengartner NW, Castillo-Chavez C, Fenimore PW, Hyman JM. The basic reproductive number of Ebola and the effects of public health measures: the cases of Congo and Uganda. J Theor Biol. 2004 Jul 7;229(1):119-26. PubMed PMID:15178190.

30. Legrand J, Grais RF, Boelle PY, Valleron AJ, Flahault A. Understanding the dynamics of Ebola epidemics. Epidemiol Infect. 2007 May;135(4):610-21. PubMed PMID:16999875.

31. Eichner M, Dowell SF, Firese N. Incubation period of ebola hemorrhagic virus subtype zaire. Osong Public Health Res Perspect. 2011 Jun;2(1):3-7. PubMed PMID:24159443.

32. Baele G, Li WL, Drummond AJ, Suchard MA, Lemey P. Accurate model selection of relaxed molecular clocks in bayesian phylogenetics. Mol Biol Evol. 2013 Feb;30(2):239-43. PubMed PMID:23090976.

33. Stadler T. Sampling-through-time in birth-death trees. J Theor Biol. 2010 Dec 7;267(3):396-404. PubMed PMID:20851708.

34. Stadler T, Kühnert D, Rasmussen DA, du Plessis L. Insights into the Early Epidemic Spread of Ebola in Sierra Leone Provided by Viral Sequence Data. PLOS Currents Outbreaks. 2014 Oct 6. Edition 1. doi: 10.1371/currents.outbreaks.02bc6d927ecee7bbd33532ec8ba6a25f.